White emission phosphors based on Dy^{3+}-doped into anhydrous rare-earth benzenetricarboxylate complexes

Ivan G.N. Silva [a], Jiang Kai [a,b], Maria C.F.C. Felinto [c], Hermi F. Brito [a,*]

[a] Departamento de Química Fundamental, Instituto de Química da Universidade de São Paulo, Cidade Universitária, 05508-000 São Paulo, SP, Brazil
[b] Departamento de Química, Pontifícia Universidade Católica de Rio de Janeiro, Gávea, 22451-900 Rio de Janeiro, RJ, Brazil
[c] Centro de Química de Meio Ambiente, Instituto de Pesquisas Energéticas e Nucleares, CNEN, Cidade Universitária, 05508-000 São Paulo, SP, Brazil

ABSTRACT

White light emitting rare earth anhydrous complexes RE(TMA):Dy^{3+} (RE^{3+} = Y^{3+} and Lu^{3+}) containing the trimesic acid ligands (TMA) were synthesized and characterized by elemental analysis, X-ray diffraction patterns, thermogravimetric analysis and infrared spectroscopy. The crystallinity and thermostability of these luminescent materials were determined. Since the first excited triplet state (T_1: 24,000 cm^{-1}) of TMA ligand is located at higher energy than the main emitting $^4F_{9/2}$ level (21,000 cm^{-1}) of the Dy^{3+} ion, TMA can act as efficient luminescent sensitizer in the intramolecular energy transfer of RE(TMA):Dy^{3+} material. The near-white emission colour originated from the intraconfigurational transitions of Dy^{3+} ion $^4F_{9/2} \rightarrow {}^6H_J$ is discussed.

© 2012 Elsevier B.V. All rights reserved.

1. Introduction

The carboxylate complexes have been gaining ground in the area of coordination compounds in the past decades due to the variety of their molecular structures which enables different chemical applications in solid state as gas storage molecular devices [1], nanostructured magnetic materials [2]. These properties allow the construction of a wide range of coordination compounds and their widespread use in many areas of knowledge, such as synthesis precursor materials [3], biomarkers [4], and optical markers [5].

Rare earth ions (RE) have been widely used as emitting centres in luminescent applications, such as organic light emitting devices (OLEDs) [6], emergency signalling [7], luminescent markers [8] and display panels [9]. Some of the RE^{3+} ions exhibit visible emission, for example, the Eu^{3+}, Tb^{3+} and Tm^{3+} ions emit in the red, green and blue region, respectively [10]. The RE^{3+} luminescence properties depend mainly on the electronic energy level structures that are little affected by their chemical environments owing to the effective shielding of the 4f electrons by the filled 5s and 5p external sub-shells [11]. Furthermore, to overcome the small molar absorptivity coefficients (<1 L mol^{-1} cm^{-1}) of the RE^{3+} ions, the coordination ligands such as carboxylate and β-diketonate groups are widely used, mainly because of their high absorptivity coefficient and luminescence sensitising abilities. This phenomenon is often denoted as the *antenna effect*, largely used in the design and synthesis of luminescent complexes [12].

From the point of view of RE^{3+} optical characteristics, Dy^{3+} (4f^9) ion has relatively large energy gap between their $^4F_{9/2}$ emitting and ^6H_J ground levels. The first triplet state (T_1) position of TMA ligand is around 24,000 cm^{-1}, which is above the emitting $^4F_{9/2}$ level (~21,000 cm^{-1}) of the Dy^{3+} ion [13], permitting the ligand-to-metal energy transfer in the TMA complexes. On the other hand, Y^{3+} (4d^0) and Lu^{3+} (4f^{14}) ions exhibit no luminescence originated from the 4f intraconfigurational transitions. In addition, the Y(TMA) and Lu(TMA) complexes present no water molecules in the coordination sphere as a result of the smaller ionic radii of Y^{3+} and Lu^{3+} cations [14]. Therefore, trivalent dysprosium ion and RE(TMA) complexes were selected in the present study as the optical activator and host matrices, respectively.

It is reported the synthesis, characterization and optical properties of the non-doped RE(TMA) and doped RE(TMA):Dy^{3+}(x%) materials (RE^{3+}: Y and Lu; x: 0.1%, 0.5%, 1.0%, 5.0% and 10% mol) in this work. Photoluminescence data were obtained from the excitation and emission spectra and lifetimes measurements. The non-radiative energy transfer from the excited triplet state (T) of TMA ligand to the emitting $^4F_{9/2}$ level of the Dy^{3+} ion as function of concentration (x% mol) were also investigated. The RE(TMA):Dy^{3+}(x%) phosphors yield white-light emission.

2. Experimental section

2.1. Synthesis of the doped RE(TMA) system

The RE^{3+} chlorides were obtained from their respective oxides RE$_2$O$_3$ (Cstarm, 99.99%) by digestion of its aqueous suspension

---

with the addition of concentrated hydrochloric acid until pH reaches 6. $RECl_3 \cdot (H_2O)_6$ crystals were obtained and dried by water bath and afterwards stored under reduced pressure.

The trimesic acid (benzene-1,3,5-tricarboxylic acid – Fluka, 97%), $H_3(TMA)$ (Fig. 1), was used without further purification. Considering the RE^{3+} ions as hard acids, the binding of these ions with carboxylates (hard base) is favoured because of their high negative charge density [15]. Since the pKa's of the $H_3(TMA)$ are 3.12, 3.89 and 4.70 [16], its aqueous solution was prepared by the addition of 1 M sodium hydroxide solution until pH reached ~6.0. At this condition, all carboxylate groups are deprotonated.

For the preparation of the doped $RE(TMA):Dy^{3+}(x\%)$ materials, 50 mL of $RECl_3$ (~0.050 M) aqueous solution of Y^{3+} or Lu^{3+}, with the required molar ratio of Dy^{3+} (0.1%, 0.5%, 1.0%, 5.0% and 10%) was dripped slowly (~1 drop per second) over 200 mL of previously prepared $(TMA)^{3-}$ ligand aqueous solution (~0.0125 M) at boiling point at molar ratio 1:1. The reaction was refluxed for about 4 h and the resulting precipitate was filtered and washed with distilled water four times. The obtained complexes are air-stable and non-hygroscopic white crystalline powders. Besides, the complexes are insoluble in different solvents such as acetone, alcohol, DMSO, acetonitrile, chloroform, water or their mixtures [17].

2.2. Characterization techniques

Elemental analysis was performed in Perkin-Elmer CHN 2400. The infrared absorption spectra were performed using KBr pellets, with the equipment Bomem MB100 FTIR in the spectral region from 400 to 4000 cm^{-1}. The X-ray diffraction patterns were recorded by a Miniflex Rigaku (Cu Kα1) from 4° to 60° (2θ). Thermogravimetry curves were obtained with the 2950 TGA HR V5.4A equipment from 30 to 900 °C in a dynamic atmosphere of synthetic air with constant heating ramp of 5 °C min^{-1}.

The photoluminescence study was conducted based on the excitation and emission spectra recorded at room temperature and 77 K, using the front-face data collection mode (22.5°), utilizing a 450 W Xenon lamp as excitation source coupled to the equipment SPEX-Fluorolog 2 with double monochromators. With a 150 W pulsed lamp attached to the phosphorimeter SPEX 1934D accessory, photoluminescence decay curves were recorded.

3. Results and discussion

The chemical composition of the RE^{3+}–TMA system determined by elemental analysis and calculated values are presented in Table S01. These results confirm the general 1:1 ratio between the TMA ligand and RE^{3+} ions and the absence of the coordinated water molecules in the $RE(TMA):Dy^{3+}(x\%)$ system.

The IR spectras were registered at room temperature and presented in Fig. S01. The symmetric $\nu_s(C=O)$ and asymmetric $\nu_{as}(C=O)$ stretching modes of the carboxylate group of the TMA

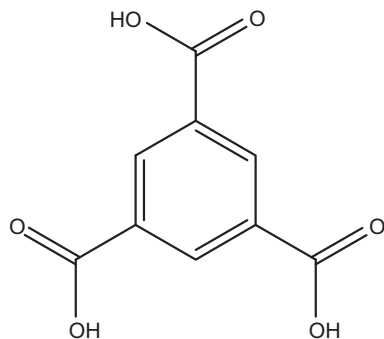**Fig. 1.** Structural formula of the 1,3,5-benzenetricarboxylic acid – $H_3(TMA)$.

ligand are observed in the spectral range from 1400 to 1600 cm^{-1}. The $\Delta\nu$ for $Na_3(TMA)$ is 195 cm^{-1}; the $\Delta\nu$ values of $RE(TMA):Dy^{3+}(x\%)$ materials are in the range of 150 to 160 cm^{-1}, indicating bridge-type coordination [18]. The sharp band observed in the infrared spectra of the $Y(TMA):Dy^{3+}(x\%)$ and $Lu(TMA):Dy^{3+}(x\%)$ samples around 3075 cm^{-1} is assigned to C—H bond stretching (Fig. S01). Besides, three sharp absorption bands were identified between 690 and 780 cm^{-1} which correspond to the out-of-plane C—H bending of the aromatic ring [19]. These IR spectral profiles are characteristics of anhydrous RE(TMA) materials.

The powder X-ray diffraction patterns of the doped and non-doped complexes are similar (Fig. 2). In addition, they present resemblances to the X-ray data for the Dy(TMA), Y(TMA) and $Y(TMA):Eu^{3+}$ anhydrous complexes reported by Serre et al. [20] and for the $Y(TMA) \cdot (H_2O)_6$ hydrated coordination compound reported by Daiguebonne et al. [21]. Whereas these X-ray diffraction patterns show small differences in the intensity and peak positions, except for the different intensity ratios between the diffraction peaks possibly due to the platelet-shaped of the samples and the presence of a peak around 26°. Furthermore, when the Dy^{3+} doping concentration changes, the diffraction peaks assigned to the Y(TMA) and Lu(TMA) host matrices show no displacement or formation of new diffraction patterns. These results also indicated the formation of a solid solution between the Dy^{3+} ion dopant and the RE^{3+}–matrices (RE^{3+}: Y and Lu) due to the similarity between the radii of rare earth ions (Fig. 2).

Fig. 3 shows the thermogravimetric curves of $RE(TMA):Dy^{3+}(x\%)$ system, which present no weight-loss event in the temperature range from 30 to 450 °C, indicating good thermal stability of the samples. This can be explained by the formation of metal–organic framework between the RE^{3+} ions and the TMA ligand. The nonappearance of the weight-loss event corresponding to the release of water molecules in this temperature interval also confirms that the $RE(TMA):Dy^{3+}$ system are anhydrous, corroborating the elemental analysis. On the other hand, in the temperature interval of 450 to 600 °C, the doped system presents only one single-step decomposition of the organic moiety, resulting in the formation of their respective sesquioxides (RE_2O_3).

4. Photoluminescent study

It is noteworthy to mention that the Dy^{3+} ion has an odd-electron configuration ($4f^9$). Therefore, it is labelled as a Kramer ion due to its electronic states that are at least doubly degenerate for any crystal-field perturbation. The maximum number of the Stark components for Kramer ions with $^{2S+1}L_J$ states is $J + 1/2$ for any symmetry lower than cubic [22].

The excitation spectra of the $Y(TMA):Dy^{3+}(x\%)$ system with emission monitored at 577 nm corresponding to the $^4F_{9/2} \rightarrow {}^6H_{13/2}$ transition of the Dy^{3+} ions are shown in Fig. 4 (left). The broad absorption band centered at 300 nm which is assigned to the TMA ligand is more intense than the narrow absorption peaks arising from 4f intraconfigurational transitions of the Dy^{3+} ion [17]. With the increased Dy^{3+}-doping, the 4f–4f transitions become more pronounced. From the position of these absorption bands originated from the $^6H_{15/2}$ ground state of the Dy^{3+} ion, the excited energy levels can be attributed as the following (in cm^{-1}): $^4F_{9/2}$ (21,230); $^4I_{15/2}$ (22,269); $^4G_{11/2}$ (23,585); $^4M_{21/2}$ (25,316); $^4K_{17/2}$, $^4F_{7/2}$, $^4I_{13/2}$ (25,974); $^4M_{11/2}$ (26,523); $^6P_{5/2}$ (27,548); $^4I_{11/2}$ (28,011), $^4M_{11/2}$, $^6P_{7/2}$ (28,653); $^4F_{5/2}$, $^4I_{9/2}$ (29,673) and $^6P_{3/2}$ (30,864) (Fig. 4 right). As can be observed, the $^6H_{15/2} \rightarrow {}^6P_{5/2}$ transition (27,548 cm^{-1}) exhibits the highest intensity among the $4f^9$ intraconfigurational transitions, indicating that in this case the direct excitation can be also used these transition from the dysprosium ion.
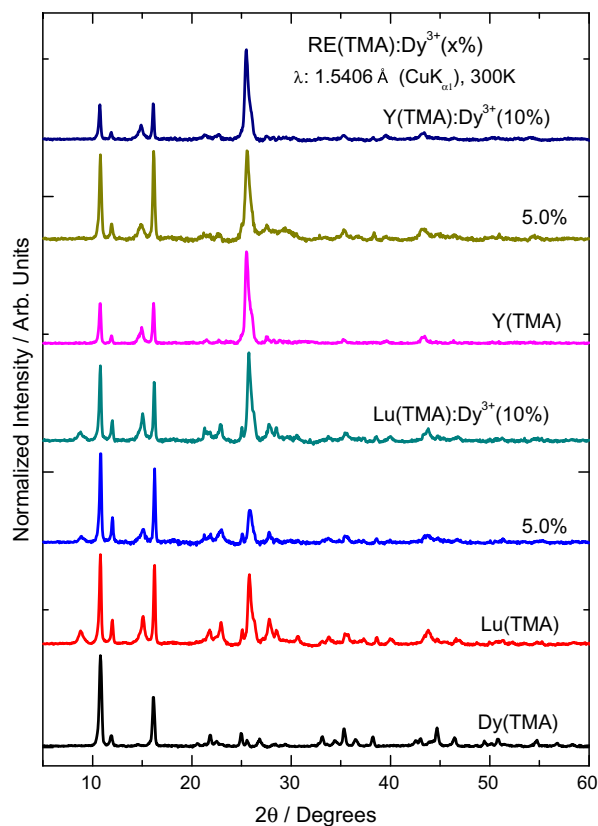
Fig. 2. X-ray powder diffraction patterns of the non-doped complexes and doped RE(TMA):Dy^{3+}(x%) system (RE: Y^{3+}, Dy^{3+} and Lu^{3+}; x: 5.0% and 10%).
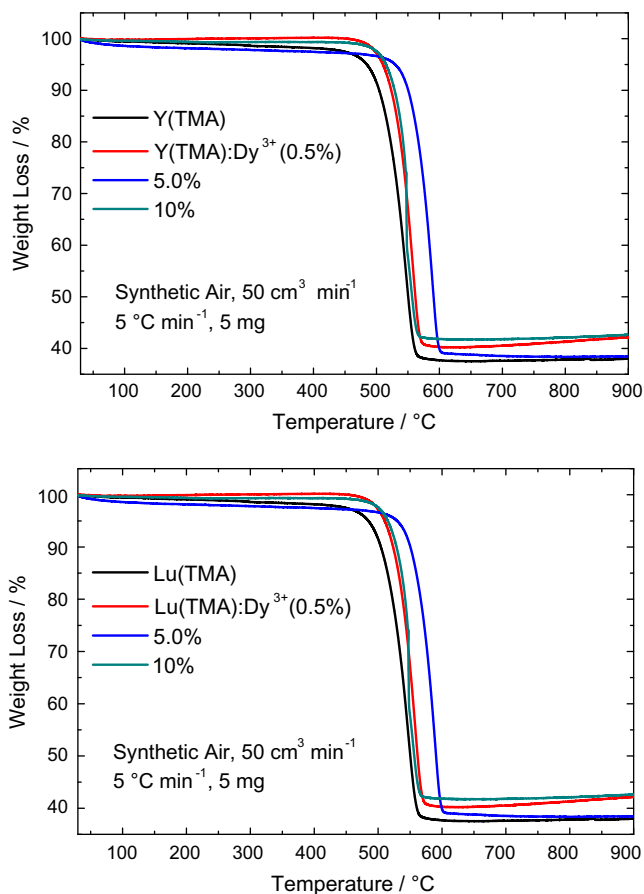

Fig. 3. Thermogravimetric curves of solid samples Y(TMA):Dy^{3+}(x%) (top) and Lu(TMA):Dy^{3+}(x%) (down). All curves were recorded in dynamic synthetic air atmosphere.

These spectroscopic results suggest an efficient intramolecular energy transfer from the TMA ligand to the Dy^{3+} ion [23]. The excitation spectra of Lu(TMA):Dy^{3+} system, as well as the spectra registered at 300 K, display very similar profiles compared to the Y^{3+} based complexes and are shown in the Fig. S02.

One important fact is that the Dy(TMA) complex does not exhibit emission bands assigned to the Dy^{3+} ion in the spectral range of 400–800 nm. This optical behaviour is owing to the nature of small energy differences between the energy levels of dysprosium ion, resulting in luminescence predominantly in the infrared range. The luminescence is also greatly quenched by the cross relaxation mechanism, which is favoured by the short distance between the Dy^{3+} ions due to the bridge-type coordination of the TMA ligand.

However, the Y(TMA) and Lu(TMA) complexes exhibit no luminescence arisen from the RE^{3+} ions due to the vacant or completely filled 4f subshell of the Y^{3+} and Lu^{3+} ions, respectively [14]. By doping the Dy^{3+} into the RE(TMA) matrices with a relatively low concentration, the inter-system crossing is reduced as the Dy^{3+} ions are well dispersed and separated, providing an increased physical distance between the Dy^{3+} ions, subsequently reducing the non-radiative decay pathways [23]. Therefore, the desired luminescence can be fine-tuned and enhanced.

The emission spectra of the RE(TMA):Dy^{3+} system (RE = Y^{3+} and Lu^{3+}) at liquid nitrogen temperature were recorded and shown in Fig. 5. The emission spectra are dominated by the $^4F_{9/2} \rightarrow {}^6H_{15/2}$ ($\sim$20,620 cm^{-1}) and $^4F_{9/2} \rightarrow {}^6H_{13/2}$ ($\sim$17,240 cm^{-1}) transitions originated from the Dy^{3+} ions in the visible region, yielding the near-white emission colour. Besides, the $^4F_{9/2} \rightarrow {}^6H_{11/2}$ ($\sim$14,930 cm^{-1}) and $^4F_{9/2} \rightarrow {}^6H_{9/2}$, $^6F_{11/2}$ ($\sim$13,240 cm^{-1}) transitions can be observed, however, with low emission intensities. It is observed that the emission spectra of Y(TMA):Dy^{3+} system (Fig. 5, left) are very similar with those recorded for the Lu^{3+} ion (Fig. 5, right), suggesting

that both rare earth ions can act as excellent luminescent matrices for this compounds. The emission spectra recorded at room temperature are shown in Fig. S03. They exhibit similar profiles with decreased peak-resolution due to increased vibronic contribution.

The absence of broadened phosphorescence band of the TMA ligand in the blue region ($\sim$450 nm) for the RE(TMA):Dy^{3+} system recorded at 77 K is more evident for compounds with doping concentration of Dy^{3+} ion from 0.5% to 10% (Fig. 5). When the spectra were recorded at room temperature (Fig. S03), the emission band from TMA ligand is not observed even at lower Dy^{3+}-doping concentration (0.1%), suggesting that energy transfer from the lowest triplet state of the TMA ligand to the dysprosium ion is very efficient.

The lifetimes (τ) of the emitting $^4F_{9/2}$ level of the Dy^{3+} ion were determined by first order exponential fitting of the photoluminescence decay curves registered at 300 K, monitoring the excitation and emission at 450 and 577 nm, respectively (Table 1). As the Dy^{3+}-doping increases from 0.1% to 10%, the lifetime values decrease slightly, from 0.37 to 0.20 ms (Fig. 6). This results can be explained by the fact that the Dy^{3+} ions are well-dispersed in the RE(TMA) matrices, therefore the lifetimes of the emitting $^4F_{9/2}$ level is relatively higher due to smaller cross relaxation. When the Dy^{3+}-doping concentration increases, the lifetime is quenched by concentration due to increased degree of cross relaxation. Besides, the longer lifetime values of the emitting $^4F_{9/2}$ level in the anhydrous RE(TMA):Dy^{3+} system are also associated with the absence of nonradiative decay channel induced by the vibronic coupling of the O—H oscillators of the water molecules [22]. Fig. 6.
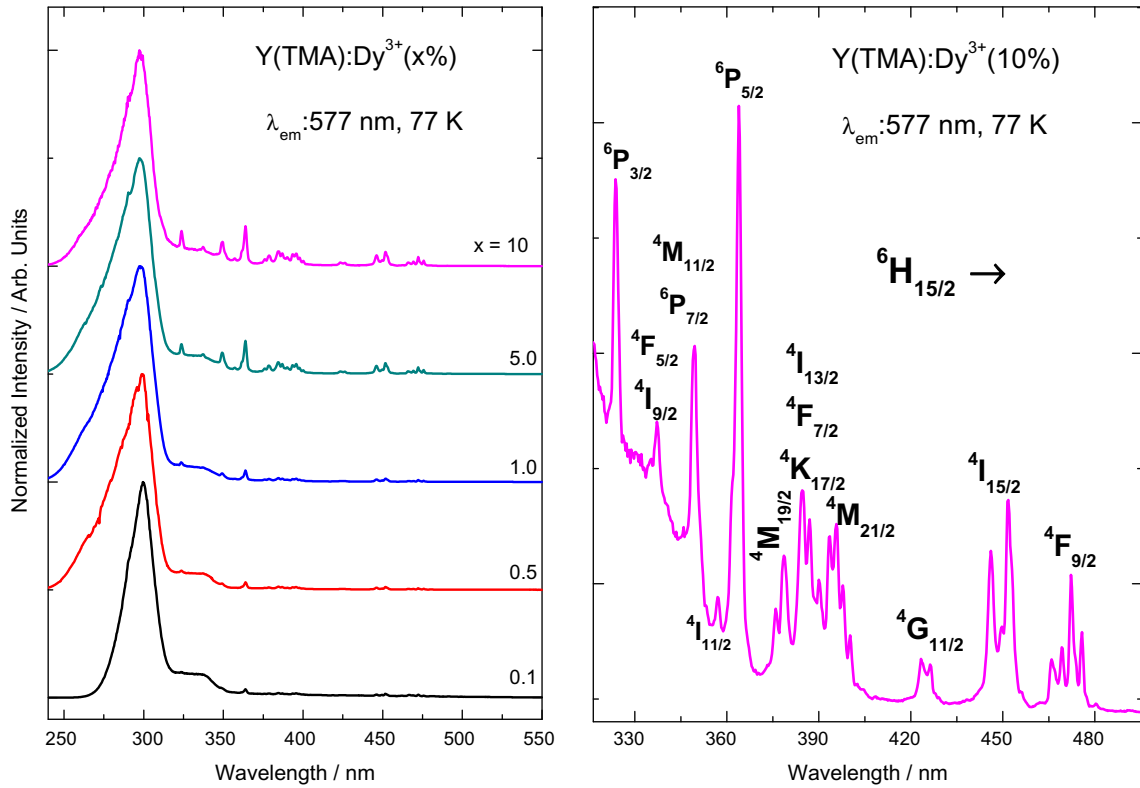
Fig. 4. The excitation spectra of the Y(TMA):Dy^{3+}(x%) system (left) and magnified peaks for the Dy^{3+}(10%)-doped compound (right) recorded at 77 K, monitoring $^4F_{9/2} \rightarrow {}^6H_{13/2}$ transition (577 nm).
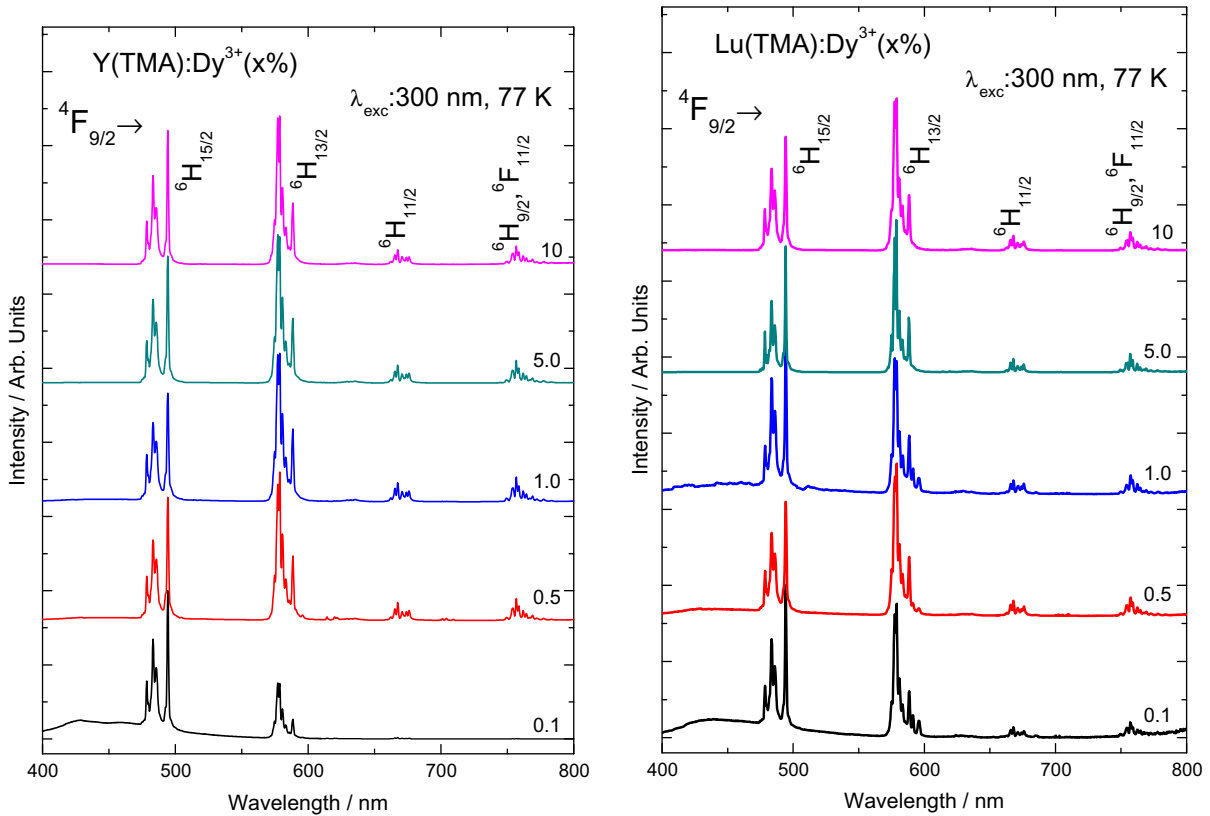

Fig. 5. Emission spectra of the doped Y(TMA):Dy^{3+}(x%) (left) and Lu(TMA):Dy^{3+}(x%) (right) system recorded at 77 K, under excitation at 300 nm.

Table 1
Lifetimes (τ) of the excited $^4F_{13/2}$ state of RE(TMA):Dy^{3+} system.

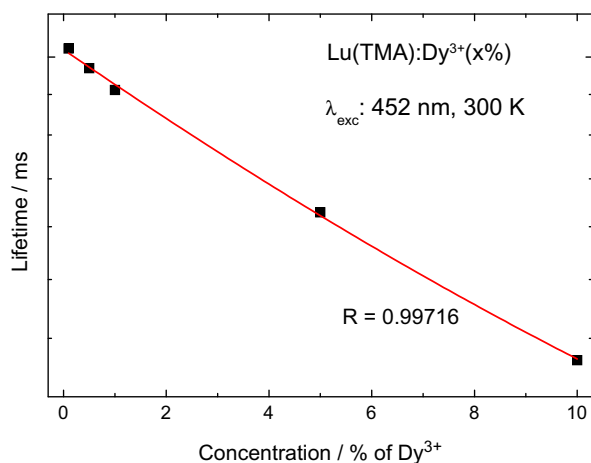| Doping concentration (%)	Lifetimes	
	Y(TMA):Dy^{3+} (ms)	Lu(TMA):Dy^{3+} (ms)
0.1	0.370	0.374
0.5	0.362	0.360
1.0	0.357	0.345
5.0	0.272	0.272
10	0.225	0.204

Fig. 6. Lu(TMA):Dy^{3+}(x%) lifetimes *versus* dysprosium doping concentrations (x: 0.1%, 0.5%, 1.0%, 5.0% and 10%).
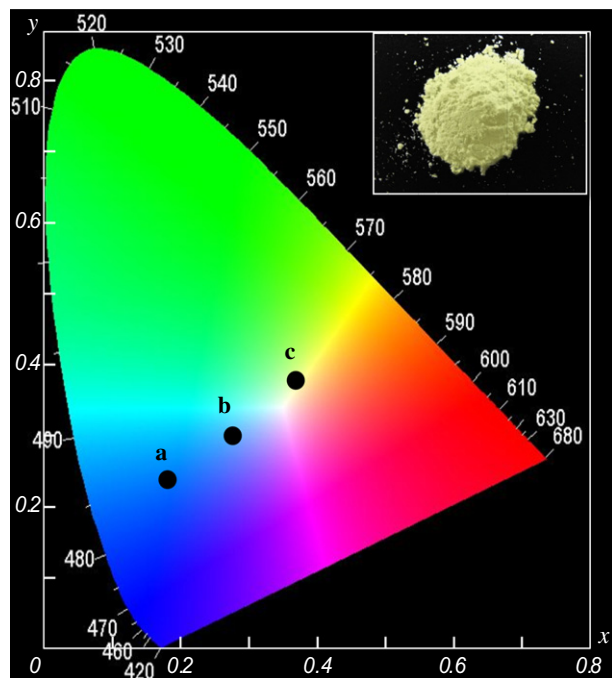

Fig. 7. CIE chromaticity diagram showing the x,y emission colour coordinates for: (a) Y(TMA):Dy^{3+}(0,1%), (b) Lu(TMA):Dy^{3+}(0.1%) and (c) RE(TMA):Dy^{3+}(x%) (x: 0.5%, 1.0%, 5.0% and 10%; RE^{3+}: Y and Lu). The inset figure is of the Y(TMA):Dy^{3+}(5.0%) powder taken with a digital camera displaying the near-white emission colour, under UV irradiated at 254 nm.

The emission colour chromaticity of these RE(TMA):Dy^{3+} complexes was studied and the CIE (*Commission Internationale de l'Éclairage*) diagram is presented in Fig 7. It is important to mention that the emission colour is independent to the Dy^{3+} doping concentration and most phosphors present the same coordinates (0.373, 0.379) in the CIE diagram [24]. This result indicates that the RE(TMA):Dy^{3+} rare earth phosphors exhibits near-white emitting colour.

5. Conclusion

Dy^{3+}-doped anhydrous Y(TMA) and Lu(TMA) inorganic matrices were synthesized using an aqueous reaction. Under the UV excitation at the ligand absorption band, the resulting insoluble luminescent materials exhibit strong near-white emission arising from the $^4F_{9/2} \rightarrow {}^6H_{15/2}$ and $^4F_{9/2} \rightarrow {}^6H_{13/2}$ intraconfigurational transitions of the Dy^{3+} ions. Combined with their excellent thermal stability, these complexes can be considered as promising candidates for white-light emitting phosphors.

Appendix A. Supplementary material

Supplementary data associated with this article can be found, in the online version, at http://dx.doi.org/10.1016/j.optmat.2012.12.001.

References

[1] U. Mueller, M. Schubert, F. Teich, H. Puetter, K. Schierle-Arndt, J. Pastre, J. Mater. Chem. 16 (2006) 626–636.
[2] E. McInnes, S. Piligkos, G. Timco, R. Winpenny, Coord. Chem. Rev. 249 (2005) 2577–2590.
[3] M. Kakihana, M. Arima, M. Yoshimura, N. Ikeda, Y. Sugitani, J. Alloys Compd. 283 (1999) 102–105.
[4] J. Shen, L.D. Sun, C.H. Yan, Dalton Trans. 42 (2008) 5687–5697.
[5] P.C.R.S. Santos, L.C. Silva, F.A.A. Paz, R.A.S. Ferreira, J. Rocha, T. Trindade, L.D. Carlos, H.I.S. Nogueira, Cryst. Growth Des. 8 (2008) 2505–2516.
[6] J. Kido, Y. Okamoto, Chem. Rev. 102 (2002) 2357–2368.
[7] J. Hölsä, T. Laamanen, M. Lastusaari, M. Malkamäki, P. Novák, J. Lumin. 129 (2009) 1606–1609.
[8] P. Gawryszewska, J. Sokolnicki, J. Legendziewicz, Coord. Chem. Rev. 249 (2005) 2489–2509.
[9] K. Binnemans, Chem. Rev. 109 (2009) 4283–4374.
[10] V.S. Sastri, J.C. Bunzli, J.R. Perumareddi, V.R. Rao, G.V.S. Rayudu, Modern aspects of rare earths and their complexes, Elsevier, Amsterdam, 2003.
[11] G.F. de Sá, O.L. Malta, C.D. Donega, A.M. Simas, R.L. Longo, P.A. Santa-Cruz, E.F. Silva, Coord. Chem. Rev. 196 (2000) 165–195.
[12] N. Sabbatini, M. Guardigl, J.M. Lehn, Coord. Chem. Rev. 123 (1993) 201–228.
[13] J. Hölsä, R.J. Lamminmäki, P. Porcher, P. Dereń, W. Stręk, Spectrochim. Acta Part A 54 (1998) 2189–2195.
[14] H.F. Brito, O.L. Malta, M.C.F.C. Felinto, E.E.S. Teotonio, The Chemistry of Metal Enolates, Luminescence Phenomena Involving Metal Enolates, John Wiley & Sons, England, 2009. pp. 131–184.
[15] L.H.J. Karhu, Anal. Chim. Acta 380 (1999) 105–111.
[16] H.C. Brown, D.H. McDaniel, O. Häfligler, F.C. Nachod, E.A. Braude, Determination of Organic Structures by Physical Methods, Academic Press, New York, 1962.
[17] E.R. Souza, I.G.N. Silva, E.E.S. Teotonio, M.C.F.C. Felinto, H.F. Brito, J. Lumin. 130 (2009) 283–291.
[18] K. Nakamoto, Infrared and Raman Spectra of Inorganic and Coordination Compounds, John Wiley & Sons, New York, 1997.
[19] R. Lyszczek, J. Therm. Anal. Calorim. 90 (2007) 533–539.
[20] C. Serre, F. Millange, C. Thouvenot, N. Gardant, F. Pelle, G. Ferey, J. Mater. Chem. 14 (2004) 1540–1543.
[21] C. Daiguebonne, O. Guilloa, Y. Gerault, A. Lecerf, K. Boubekeur, Inorg. Chim. Acta 284 (1999) 139–145.
[22] W.T. Carnall, P.R. Fields, K. Rajnakt, J. Chem. Phys. 49 (1968) 4424–4442.
[23] R.E. Whan, G.A. Crosby, J. Mol. Spectrosc. 8 (1962) 315–327.
[24] P.A. Santa-Cruz, F.S. Teles, Spectra Lux Software vol. 2.0 Beta, Ponto Quântico Nanodispositivos, RENAMI, 2003.